Journal for Geometry and Graphics
Volume 8 (2004), No. 2, 171–183.

# Error Propagation through Geometric Transformations

**Shi-Min Hu**[1], **Johannes Wallner**[2]

[1] *Dept. of Computer Science and Technology, Tsinghua University, Beijing*
*email: shimin@tsinghua.edu.cn*

[2] *Inst. f. Diskrete Mathematik und Geometrie, TU Wien*
*Wiedner Hauptstr. 8-10/104, 1040 Vienna, Austria*
*email: wallner@geometrie.tuwien.ac.at*

**Abstract.** We investigate the propagation of errors through geometric transformations, such as reflections, rotations, similarity transformations, and projections, and also the scalar product of vectors. This means computing tolerance zones of points which undergo such transformations, if these points and the transformations themselves are given by toleranced input data.

*Keywords:* Error propagation, geometric transformation, tolerance zone
*MSC 2000:* 51M04

## 1. Introduction

Geometric objects whose precise location is undefined but are known to be contained in some *tolerance zone*, are the basic entities of robust geometric computing for Computer-Aided Design. Starting with interval arithmetic [1, 5, 6, 7, 8, 13, 14], which represents imprecise floating point numbers by small intervals, there is a huge amount of literature which deals with the practical aspects of representation and computing with such entities [9]. In this context, *worst case tolerancing* means that some mathematical objects, which serve as an argument for some function, are given by their tolerance zones, and we seek for the set of possible outcomes, i.e., function values [12]. Interesting work has been done by C.U. Hinze [4], who analyses several elementary constructions in the Euclidean plane. An application to collision problem involving toleranced objects has been given by M. Aichinger [2]. [15] considers affine and convex combinations of points and also the circumcircle of three points from the viewpoint of error propagation. [10] further considers metric constructions and the computation of boundaries of tolerance zones. In this paper we are concerned with certain geometric transformations in the Euclidean plane. We consider the propagation of errors through toleranced geometric transformations: central similarities, reflections, projections, and the scalar product of tolerances vectors.

ISSN 1433-8157/$ 2.50 

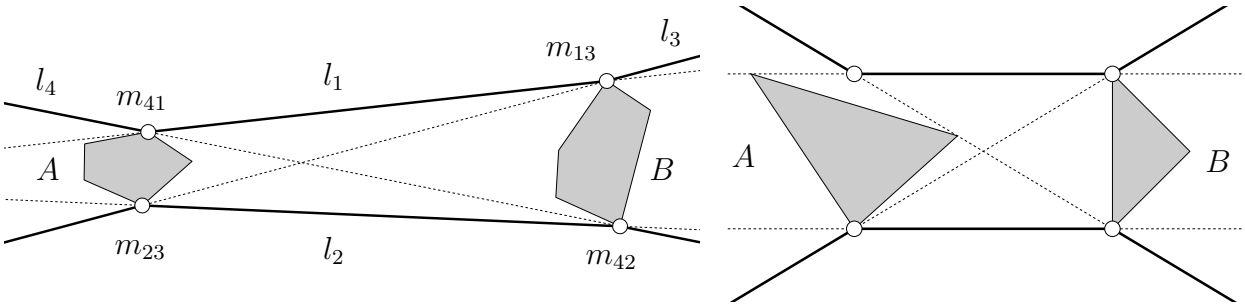


Figure 1: Fat lines with butterflies defining $|A \vee B|$

## 2. Preliminaries

### 2.1. Fat points and fat lines

In Euclidean geometry, *points* are the most elementary geometric objects. A *fat point* is a set of points. Usually when computing with fat points, one restricts attention to sets with certain properties, like closed convex ones, or even balls. In general, small letters denote geometric objects, and capital letters denote their 'fat' variants. In this paper, we restrict ourselves to the case the Euclidean plane (i.e., $d = 2$).

We define a fat line by either of the two following definitions:

**Def. 1** *(Fat line, version 1) If $A, B$ are fat points, then the fat $L$ spanned by $A$, $B$ is set of lines which meet both $A$ and $B$. We write $L = A \vee B$.*

*(Fat line, version 2) For fat points $A$ and $B$, the fat line $L$ spanned by $A$, $B$ consists of all points contained in a line which meets both $A$ and $B$. We write $|L| = |A \vee B|$.*

Two lines which are not parallel dissect the plane into four closed *angular domains*, which fall into two pairs of *opposite* ones (see Fig. 1, left). Two parallel lines dissect the plane into three closed regions (see Fig. 1, right), one of which contains the two lines and is called, for the sake of consistency, an angular domain also. The following is elementary:

**Prop. 1** *Suppose that the fat points $A$ and $B$ have two exterior common tangents $l_1, l_2$ with the property that both $A$ and $B$ are contained in an angular domain bounded by $l_1$ and $l_2$; and suppose further that $A$ and $B$ have two interior common tangents $l_3, l_4$, with the property that $A$ is contained in an angular domain bounded by $l_3$ and $l_4$ and $B$ is contained in the opposite one. Then the union of these three angular domains equals $|A \vee B|$.*

Clearly the assumptions of Prop. 1 are fulfilled if both $A$ and $B$ are disjoint and convex, or are contained in disjoint convex sets (see Fig. 1). We call the four lines the *butterfly structure* defined by the fat points $A$ and $B$. The lines contained in the region $|A \vee B|$ may be or may not be the lines of $A \vee B$. Examples for this behaviour are seen in Fig. 1 left and right.

### 2.2. Minkowski sum

We will employ the Minkowski sum operation: If $A$ and $B$ are subsets of $\mathbb{R}^2$, their *Minkowski sum* is defined by $A + B = \{a + b \mid a \in A, b \in B\}$.

For convex *polygons*, the Minkowski sum is computed easily [3]: Assume that, up to parallel translations, the boundaries of $A$ and $B$ are given by concatenation of edges $e_1^A, \ldots, e_k^A$ and $e_1^B, \ldots, e_l^B$, respectively. These two lists are sorted by angle. Then the boundary of $A+B$

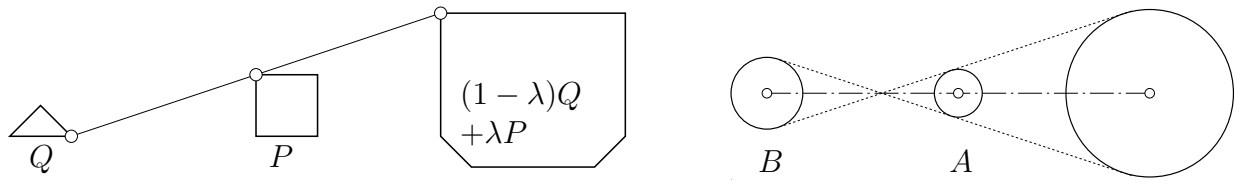


Figure 2: Left: Central similarity with center $Q$ and factor $\lambda = 2$.
Right: Reflection of a disk in a disk

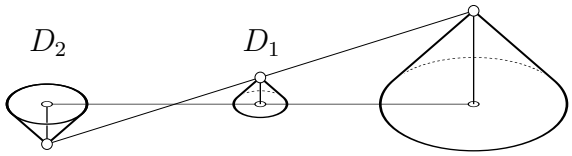


Figure 3: Cyclographic interpretation of reflection

is given, up to a parallel translation, by the concatenation of the list of edges which arises from merging the two previous lists and sorting by angle.

Note that if an edge of $A$ is parallel to an edge of $B$, that is, both the edges have the same outer normal direction, their lengths are added automatically by the concatenation process.

## 3. Central similarities

For a given point $o$, the transformation $x \to o + \lambda \cdot \overrightarrow{ox} = (1-\lambda)o + \lambda x$ is called the *central similarity* transformation with center $o$ and factor $\lambda$. The special case $\lambda = -1$ is the *reflection in o*.

If $P$, $Q$ are fat points, the central similarity of $P$ with center $Q$ and factor $\lambda$ is given by the set $(1-\lambda)Q + \lambda P$. In the case that both $P$ and $Q$ are bounded by convex polygons, this Minkowski sum may be computed by the algorithm mentioned in Sect. 2.2. See Fig. 2 for an example.

If a central similarity is defined by fat *disks* $A = D(c, r)$ and $B = D(c', r')$ with centers $c, c'$ and radii $r, r'$, resp., then the result is the disk $(1-\lambda)D(c,r) + \lambda D(c',r') = D((1-\lambda)c, |1-\lambda|r) + D(\lambda c', |\lambda| r') = D((1-\lambda)c + \lambda c', |1-\lambda|r + |\lambda|r')$. The special case of reflection ($\lambda = -1$) results in the disk $D(2c - c', 2r + r')$ (see Fig. 2).

Disks may be represented by points of three-space via the *cyclographic mapping* (see [11]): We represent an oriented circle with center $c = (x, y)$ and signed radius $r$ by the point $(x, y, r)$ in $\mathbb{R}^3$. Now the fat points $A$, $B$, and $A - (B - A)$ are represented by the three points $(x, y, r)$, $(x', y', r')$, and $(2x - x', 2y - y', 2r + r')$, respectively. These three points in space are related: Reflection of the first in the second yields the third (see Fig. 3).

## 4. Reflection in a line

In this section, we consider reflection of a fat point in a fat line of butterfly structure. Unfortunately reflection of a convex fat point in a fat line will result in a non-convex tolerance domain of the image point. It is nevertheless not difficult to compute that image point from the original fat point from the butterfly.

We denote the result of reflection of a point $p$ in line $l$ by $\rho(p, l)$. The notation "arc$(c, p, q)$"

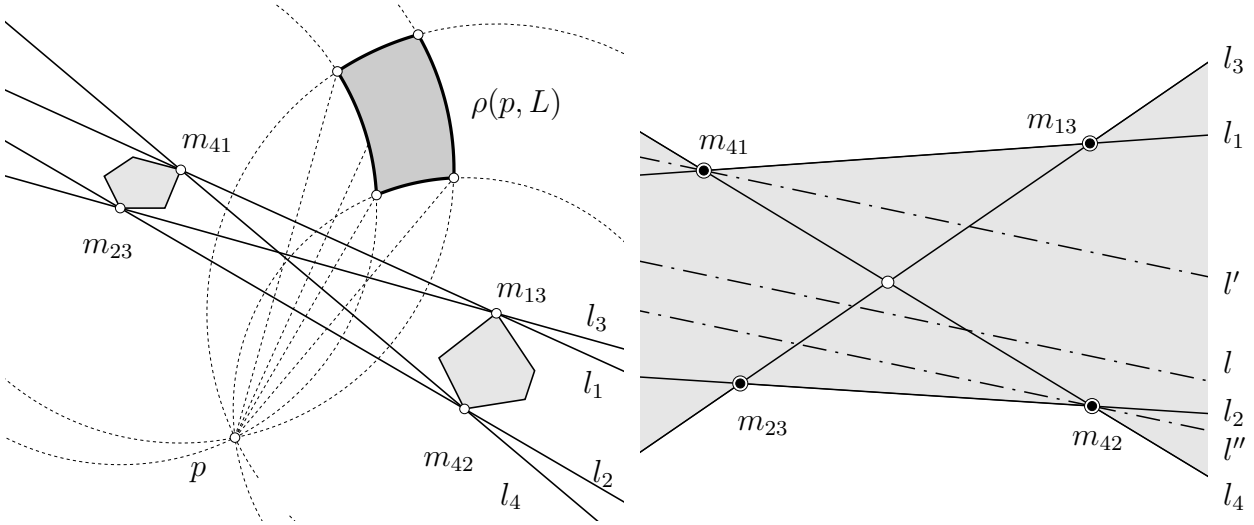


Figure 4: Left: Tolerance zone of reflection of a point in a fat line. Right: Butterfly structure

is used for the arc which is the path traversed by the point $p$ when rotated counter-clockwise into the point $q$ about the center $c$.

### 4.1. Reflection of a point in a fat line

We first consider reflection of the point $p$ in a fat line $L$ characterized by the butterfly structure consisting of the four lines $l_1, \ldots, l_4$.

**Def. 2** *(butterfly indices and wedges) The four lines $l_1, \ldots, l_4$ defining a butterfly structure have 6 intersection points $m_{ij}$, two of which are interior points, and four of which are boundary points We assume that the four points $m_{ij}$ are indexed in such a way that while rotating the line $l_i$ about the point $m_{ij}$ counter-clockwise into the line $l_j$ we stay inside the fat line. This set of lines traversed during that rotation, is called the wedge $W_{ij}$ belonging to $m_{ij}$.*

This is illustrated in Fig. 4, where the boundary points are indicated in black, and only one of the two interior points can be seen.

**Prop. 2** *If $L$ has butterfly structure, the tolerance zone $\rho(p, L)$ is the planar domain bounded by the four arcs $A_{ij} = \operatorname{arc}(m_{ij}, \rho(p, l_i), \rho(p, l_j))$, where $m_{ij}$ is a boundary point of the fat line according to Def. 2.*

*Proof.* Reflecting $p$ in all lines $l \in W_{ij}$ results in the arc $A_{ij}$. This arc belongs to a circle which passes through $p$ itself, which implies the fact that if $x \in A_{ij}$, then the line segment $\overline{xp}$ intersects $A_{ij}$ in $x$ and possibly in $p$, but in no other point.

For an arbitrary non-boundary line $l \in L$ there are exactly two lines $l'$ and $l''$ parallel to $l$ and contained in wedges $W_{ij}$ and $W_{kl}$ (see Fig. 4). The reflections $\rho(p, l')$, $\rho(p, l)$, $\rho(p, l'')$ lie on a line, in that order, and this line contains $p$.

Thus we have shown that the set of all possible reflections $\rho(p, l)$ is the union of all possible line segments $\overline{\rho(p, l')\rho(p, l'')}$. These intersect each of four arcs in the points $\rho(p, l')$ and $\rho(p, l'')$, and possibly in $p$ itself, and their carrier lines are incident with $p$. Thus we conclude that this union is actually bounded by the four arcs $A_{ij}$. □

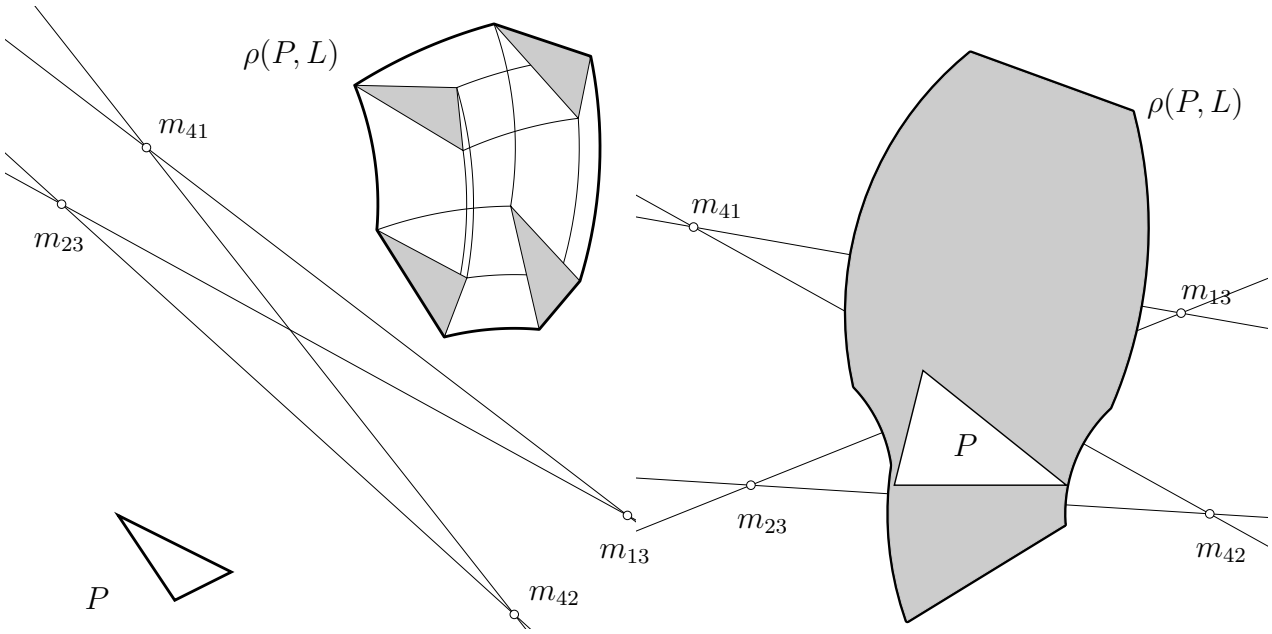


Figure 5: Left and Right: Tolerance zone of reflection of a fat point in a fat line

### 4.2. Reflection of a fat point in a fat line

If $\rho(p, L)$ denotes the reflection of a point $p$ in a fat line $L$, then the tolerance zone $\rho(P, L)$ of reflection of a fat point $P$ in the fat line $L$ is given alternatively by

$$\rho(P, L) = \bigcup_{p \in P} \rho(p, L) = \bigcup_{l \in L} \rho(P, l).$$

Algorithm 1 below computes the boundary of $\rho(P, L)$ if $P$ is a fat point without holes. The result consists of arcs and parts of the boundary of $P$ (see Fig. 5). It assumes that the lines $l_1, \ldots, l_4$ constitute the butterfly which determines the fat line $L$.

**Algorithm 1** *(Computing the boundary of $\rho(P, L)$ if $L$ has butterfly structure and $P$ has no holes):*

1. *Find boundary points $m_{ij} = l_i \cap l_j$ of the butterfly and index according to Def. 2. Compute $\rho(P, l_i)$ $(i = 1, 2, 3, 4)$.*
2. *For all four points $m_{ij}$, trace the boundary curve of $\rho(P, l_i)$ and determine points $m_r^{(ij)}$ $(r = 1, 2, \ldots)$ on the boundary of $P$ such that distance from $m_{ij}$ assumes local maxima and minima in the points $\rho(m_r^{(ij)})$.*
   (a) *special case: If $m_{ij}$ is outside $\rho(P, l_i)$ and $P$ is convex, there is exactly one maximum and one minimum.*
   (b) *special case: If $m_{ij}$ is inside $\rho(P, l_i)$ and $P$ is star-shaped with respect to $m_{ij}$ (and especially if $P$ is convex), it is sufficient to consider the maxima only.*
3. *For all points $m_r^{ij}$ found in this way, consider the arcs* $\mathrm{arc}(m_{ij}, \rho(m_r^{ij}, l_i), \rho(m_r^{ij}, l_j))$.
4. *Consider the union $M$ of all arcs found in step 3 and also the four domains $\rho(p, l_i)$. The 'inside' of $M$ is the tolerance domain we look for.*

The idea of this algorithm is to consider the path of $P$ when subject to reflection in the lines of $L$ which path through the centers $m_{ij}$ of the butterfly. Successive reflection of $P$ in

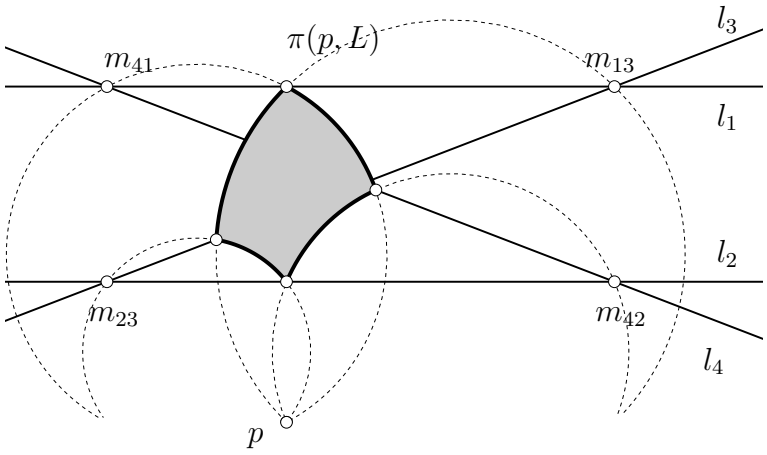


Figure 6: Tolerance zone of projection of a point onto a fat line

lines incident with $m_{ij}$ results in copies of $P$ which can be transformed into each other by rotation about $m_{ij}$. Thus we consider the four copies $\rho(P, l_i)$ and look for the domains traced out by $\rho(P, l)$ when $l$ is in $L$ and incident with $m_{ij}$. The boundary of this domain will consist of arcs and the boundaries of $\rho(P, l_i)$, $\rho(P, l_j)$ themselves (see Fig. 5).

*Proof.* (of correctness of Alg. 1) The region traced out the $\rho(P, l)$ when $l \in L$ and $m_{ij} \in l$ is bounded by $\rho(P, l_i)$, $\rho(P, l_j)$, and the some arcs. Clearly the algorithm finds all those arcs. It follows that the 'inside' of the union of the arcs belonging to $m_{ij}$ together with $\rho(P, l_i)$ and $\rho(P, l_j)$ is the domain in question. In this way we have shown that the algorithm does not exaggerate the tolerance zone $\rho(P, L)$,

We still have to show that all $\rho(p, L)$, with $p \in P$, are contained in the domain described by Alg. 1. It is clearly sufficient to show that the four boundary arcs of $\rho(p, L)$ have this property. For any $p$, each of these four arcs can be generated as the path of $p$ when reflected successively in the lines of $L$ incident with one of the four points $m_{ij}$. Therefore each of the four arcs are contained in one of the four regions considered in the previous paragraph, and we are done. □

*Remark.* If $P$ does not intersect the fat line $L$ and $P$ is convex, Algorithm 1 will find eight arcs, but only four contribute to the boundary of $\rho(P, L)$ (see Fig. 5). ♢

## 5. Projection of a point onto a line

Projection of a point $p$ onto a line $l$ occurs in many geometric computations. Here it is denoted by $\pi(p, l)$. The relation $\rho(p, l) = 2\pi(p, l) - p$ between reflection in $l$ and projection onto $l$ immediately shows

**Prop. 3** *The tolerance zone $\pi(p, L)$ where $L$ has butterfly structure is the planar domain bounded by the four arcs* $\mathrm{arc}(m_{ij}, \pi(p, l_i), \pi(p, l_j))$, *where $m_{ij}$ is a boundary point of $|L|$ according to Def. 2.*

Prop. 3 is illustrated by Fig. 6. Obviously, the projection $\pi(P, l)$ of a fat point onto a line $l$ is an interval of that line. Thanks to the simple structure of $\pi(P, l)$ we have the following result:

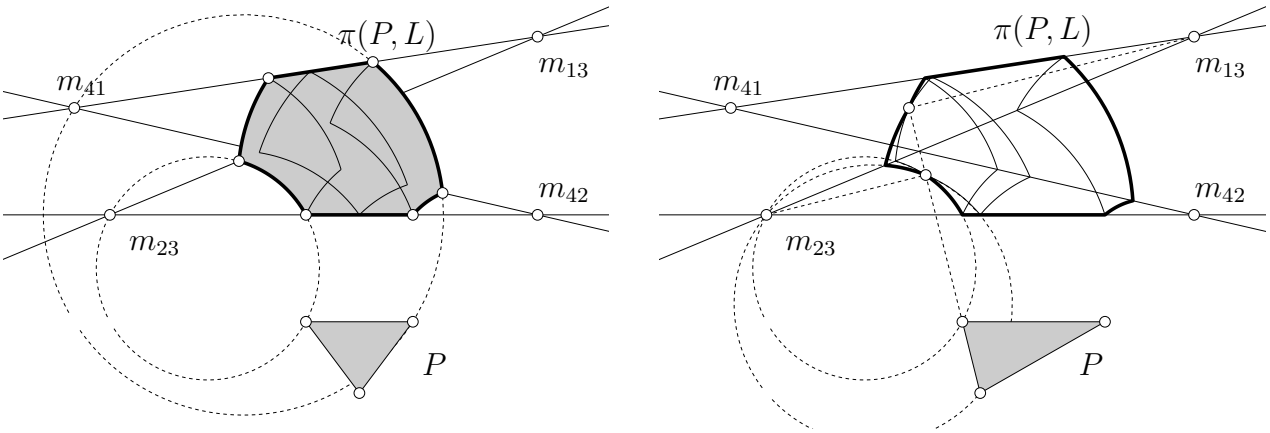


Figure 7: Projection of a fat point onto a fat line

**Prop. 4** *Assume that $P$ is a fat point and $L$ is a fat line of butterfly structure. For all wedges $W_{ij}$ according to Def. 2, and all lines $l \in W_{ij}$ onsider the projection $\pi(P,l)$, which is an interval, and mark its endpoints. Consider the eight curves of these endpoints together with the segments $\pi(P,l_i)$ $(i=1,\dots,4)$ — the interior of the region defined by these twelve curves is $\pi(P,L)$.*

*Proof.* In a way analogous to the proof of correctness of Alg. 1 we have to show that $\pi(p,L)$ is contained in the region described by the proposition. This is true because $\pi(p,L)$ is bounded by arcs (see Prop. 3) which arise from projecting $p$ onto the lines of $L$ incident with one of the points $m_{ij}$. □

*Remark.* The actual computation of $\pi(P,L)$, if $P$ is a convex polygon, is simple: Successively projecting $P$ onto the lines of $L$ which are incident with one of the point $m_{ij}$ results in a sequence of arcs, the boundary points of which lie on the lines $l_i$ and $l_k$, and also on lines incident with $m_{ij}$ and orthogonal to an edge of $P$ (see Fig. 7, right). ♢

## 6. Similarity Transformations

### 6.1. Toleranced similarity: Minkowski sum

**Def. 3** *The general similarity transformation $G(q,\theta,\lambda)$ with center $q$, angle $\theta$, and factor $\lambda$ maps a point $p$ according to*

$$p \mapsto q + \lambda A_\theta \cdot (p-q), \quad A_\theta = \begin{pmatrix} \cos\theta & -\sin\theta \\ \sin\theta & \cos\theta \end{pmatrix}. \tag{1}$$

We will show how the image of a toleranced point under a general similarity transform with toleranced center is easily computed via Minkowski sums.

First we define *complementary* similarity matrices: If $r$ is the result of applying $G(q,\theta,\lambda)$ to $p$, then there is a similarity $G(p,\theta',\lambda')$ such that $r$ also is the result of applying $G(p,\theta',\lambda')$ to $q$. The relation between the $\theta,\lambda,\theta',\lambda'$ can be seen from the triangle of Fig. 8: We have

$$\lambda' = \sqrt{1-2\lambda\cos\theta+\lambda^2}, \quad \lambda^2 = 1^2 + \lambda'^2 - 2\lambda'\cos\theta'. \tag{2}$$

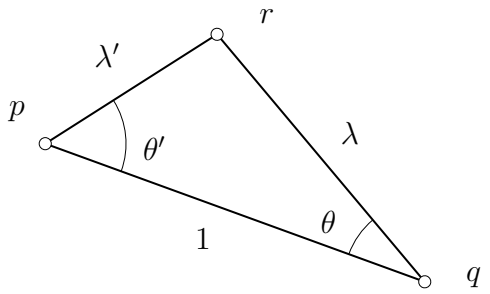


Figure 8: Complementary general similarity transformations

Obviously the relation between $\theta, \lambda, \theta', \lambda'$ involves neither center. There is also a second relation: The equations

$$r = (E - \lambda A_\theta)q + \lambda A_\theta p, \quad r = (E - \lambda' A_{\theta'})p + \lambda' A_{\theta'} q, \tag{3}$$

(where $E$ is the $2 \times 2$ identity matrix) for all $p$ and $q$ show that

$$\lambda A_\theta + \lambda' A_{\theta'} = E. \tag{4}$$

The following is a direct consequence of Equ. (3).

**Prop. 5** *If $P, Q$ are fat points, then the result of applying the general similarity $G(Q, \theta, \lambda)$ to $P$ is given by $\lambda' A_{\theta'} \cdot Q + \lambda A_\theta P$, where the relation between $\theta, \lambda$ and $\theta'$, $\lambda'$ is given by both Equ. (2) and (4).*

Prop. 5 shows that we can compute the result of a toleranced general similarity by a Minkowski sum. We have a look at the special cases $\lambda = 1$ (rotation) and $\theta = 0$ (central similarity) now.

**Prop. 6** *If $P, Q$ are fat points, then the result of applying the rotation $G(Q, \theta, 1)$ to $P$ is given by $\lambda' A_{\theta'} \cdot Q + A_\theta P$, where $\theta'$ and $\lambda'$ are given by*

$$\lambda' = 2\sin(\theta/2), \quad \theta' = \pi/2 - \theta/2. \tag{5}$$

*Proof.* This follows by letting $\lambda = 1$ in Equ. 2, or directly from Fig. 8. □

As to the central similarity, letting $\theta = 0$ results in either $\theta' = \pi$ and $\lambda' = \lambda - 1$, or in $\theta' = 0$ and $\lambda' = 1 - \lambda$, so we get the result of Sect. 3 again.

### 6.2. Toleranced similarity: Support functions

We are going to express Prop. 5 and Prop. 6 in terms of *support functions*: The real-valued $2\pi$-periodic function $s$ is the support function of the fat point $P$, if the half-space $x\cos\phi + y\sin\phi \leq s(\phi)$ contains $P$ and its boundary is tangent to $P$. It is easy to see that the rotated copy $P' = A_\theta \cdot P$, the scaled copy $P'' = \lambda P$ with $\lambda > 0$, and the reflected copy $P''' = -P$ have the support functions $s'(\phi) = s(\phi - \theta)$, $s''(\phi) = \lambda s(\phi)$, $s'''(\phi) = s(\phi + \pi)$, respectively. Equ. (2) always results in $\lambda' > 0$. It is no loss of generality if we restrict ourselves to scale factors $\lambda > 0$, because a negative factor can always be expressed by an additional rotation through 180 degrees:

$$A_\pi = -E, \quad \lambda A_\theta = (-\lambda) A_{\theta+\pi}. \tag{6}$$

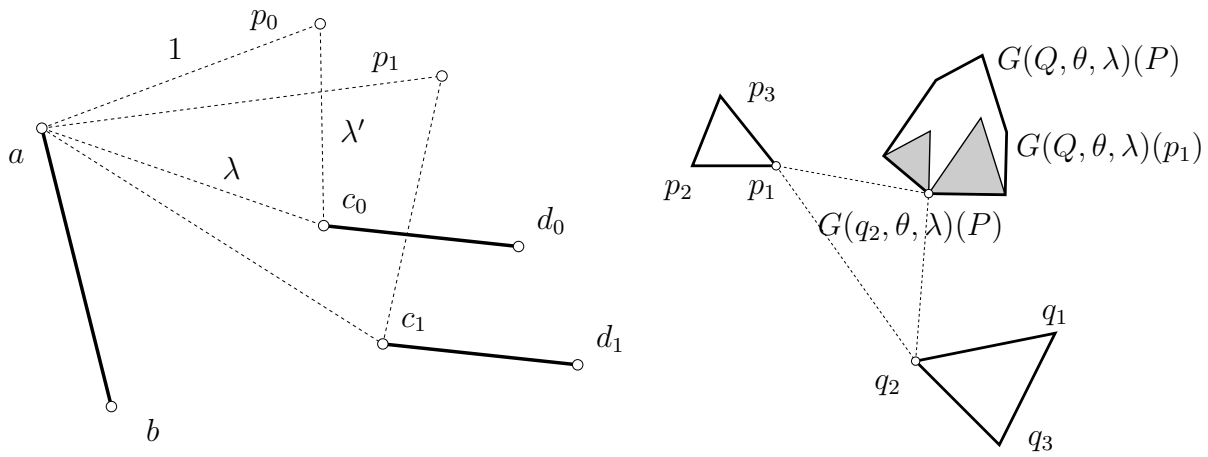


Figure 9: Left: Illustration of properties of the general similarity transformation. Right: $G(Q,\theta,\lambda)(P)$ for triangles $P$ and $Q$

Now Prop. 5 reads as follows: If $P$ and $Q$ have support functions $s$ and $s'$, resp., then the support function $s''$ of $G(P,\theta,\lambda)$ applied to $P$ is given by $s''(\phi) = \lambda' s'(\phi - \theta') + \lambda s(\phi - \theta)$, where $\lambda'$ and $\theta'$ are given by Equ. (2). The same applies to the rotation $G(P,\theta,1)$: using the explicit expressions of Equ. (5), we get $s''(\phi) = 2\sin\frac{\theta}{2} \cdot s'(\phi - \frac{\pi-\theta}{2}) + s(\phi - \theta)$.

### 6.3. Toleranced similarity: Polygons

If the fat points which define and which undergo a general similarity transform are bounded by polygons, it is not difficult to compute the polygons which occur as the results of that transformation. We can use the algorithm of Sect. 2.2 to compute the Minkowski sums mentioned in Prop. 5 and Prop. 6. It is worth to note two properties of general similarity transformations which follow directly from these two propositions, and which are illustrated in Fig. 9. $\theta, \lambda$, and $\theta', \lambda'$ belong to complementary similarities.

1. For a given point $p$ and a given line segment $\overline{ab}$, applying $G(\overline{ab},\theta,\lambda)$ to $p$ results in a line segment, and so does applying $G(p,\theta',\lambda')$ to $\overline{ab}$.
2. If $p_1,\ldots,p_n$ are points and $\overline{ab}$ is a line segment, then the images of $\overline{ab}$ under $G(p_i,\theta,\lambda)$ are parallel, and so are the images of the points $p_i$ under $G(\overline{ab},\theta',\lambda')$.

Fig. 9 shows the segments

$$\overline{c_0d_0} = G(p_0,\theta',\lambda')(\overline{ab}) = G(\overline{ab},\theta,\lambda)(p_0) \quad \text{and} \quad \overline{c_1d_1} = G(p_1,\theta',\lambda')(\overline{ab}) = G(\overline{ab},\theta,\lambda)(p_1).$$

By property 2, they are parallel. Fig. 9 also illustrates $G(Q,\theta,\lambda)$ applied to $P$, where both $P$ and $Q$ are triangles.

### 6.4. Toleranced similarity: disks

The change in size of tolerance zones is best appreciated when considering disks as tolerance zones. Prop. 5 and Prop. 6 immediately give the following result: If $P$ and $Q$ are disks of radii $r$ and $r'$, respectively, then applying the similarity with center $Q$ and parameter $\theta$, $\lambda$ to $P$ results in a disk of radius

$$r'\sqrt{1+\lambda^2-2\lambda\cos\theta} + r\lambda, \tag{7}$$

if $\lambda > 0$. Applying the rotation with center $Q$ and angle $\theta$ to $P$ results in a disk of radius

$$2r' \left|\sin(\theta/2)\right| + r. \tag{8}$$

## 7. Inner product of fat vectors

A 'fat vector', i.e., the tolerance zone of a vector, is nothing else than a fat point once an origin of a coordinate system has been specified. The sum of fat point $P$ and a fat vector $V$ is the fat point $P + V$ (Minkowski sum).

The tolerance zone $A \cdot B$ of the scalar product of two fat vectors $A$, $B$ is an interval, if both $A, B$ are compact and connected. Obviously, $A \cdot B = [\min_{x\in A, y\in B}(x \cdot y), \max_{x\in A, y\in B}(x \cdot y)]$. In order to compute $A \cdot B$ for fat vectors with smooth or piecewise smooth boundary curves we will need the concept of *tangent* of a such a curve in a point $p$. If $p$ is in the interior of a smooth part of the curve, the tangent is well defined in the usual sense. At vertices the curve is thought to be rounded off by a very small arc, and the tangents of this arc are defined to be tangents of the original curve in this vertex.

**Prop. 7** *Suppose that $A$ and $B$ are fat vectors bounded by piecewise smooth curves. Then the pairs $(x, y)$ with $x \in A$, $y \in B$ where $x \cdot y$ assumes its maximum and minimum have the property that they are contained in the respective boundaries of $A$ and $B$, and that there exist tangents $T_x$, $T_y$ such that*

$$\overrightarrow{ox} \perp T_y \quad \textit{and} \quad \overrightarrow{oy} \perp T_x. \tag{9}$$

*Proof.* The function $x \cdot y$ with both $x$ and $y$ ranging freely in $\mathbb{R}^2$ has no stationary point except at $x = y = 0$, and this is neither a maximum mor a minimum. This shows that maximum and minimum must occur at the boundaries of $A$ and $B$.

First we suppose that they can be smoothly parametrized by curves $c(t)$ and $d(s)$. A necessary condition for a maximum or minimum is that $\frac{\partial}{\partial t}(c(t) \cdot d(s)) = \dot{c}(t) \cdot d(s) = 0$, $\frac{\partial}{\partial s}(c(t) \cdot d(s)) = c(t) \cdot \dot{d}(s) = 0$. Here $\dot{c}$ and $\dot{d}$ denote derivatives. Thus we have shown condition (9). The case of piecewise smooth boundaries follows by a standard limit argument, as already indicated in the paragraph conderning the definition of 'tangent'. □

Fig. 10 illustrates condition (9) for polygons $A$ and $B$. We will however see in Prop. 8 that computing $A \cdot B$ in that case benefits from additional properties.

*Remark.* Morse theory implies the nontrivial fact that there are at least four pairs of points which satisfy condition (9): at least one maximum, one maximum, and two saddle points of the function $x \cdot y$ where $x, y$ range in the respective boundaries of $A$ and $B$, cf. [16]. ♢

**Prop. 8** *If the fat vectors $A$ and $B$ are bounded by polygons, the minimum and maximum of $x \cdot y$ with $x \in A$ and $y \in B$ occurs for vertices $x$ of $A$ and $y$ of $B$.*

*Proof.* We have to show that the function $x \cdot y$ has neither minimum nor maximum if both $x$ and $y$ range in straight lines. Thus we assume that $x(t) = a + tb$ and $y(s) = c + sd$ and get

$$x \cdot y = a \cdot c + s(a \cdot d) + t(b \cdot c) + st(b \cdot c).$$

If $b \cdot c \neq 0$ this is a quadratic function whose purely quadratic part ("$st$") has only one saddle point; and which therefore does not have a minimum or maximum; if $b \cdot c = 0$ this is a linear or even constant function, which has neither of them also. □

It is therefore possible to compute the interval $A \cdot B$ by evaluating $x \cdot y$ for all vertices $x \in A$ and $y \in B$. We may disregard vertex pairs which do not fulfill condition (9).

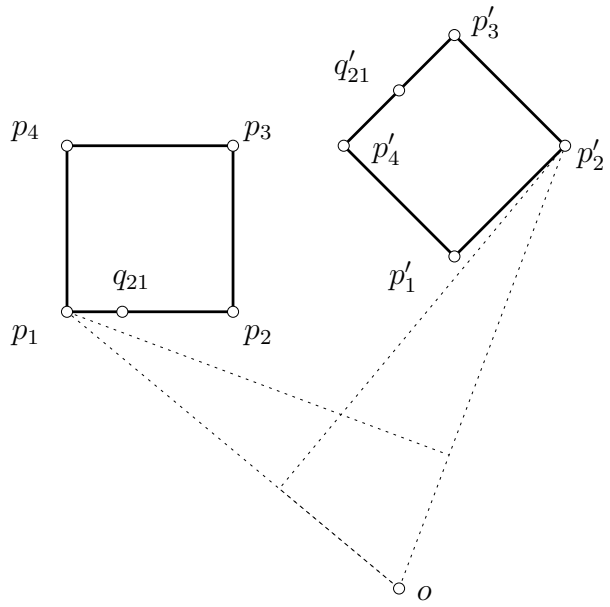


Figure 10: Pairs of points which satisfy condition (9) are $(q_{21}, q_{21}')$, $(p_1, p_2')$, $(p_3, p_1')$, and $(p_3, p_3')$

## 8. Cumulation of errors

When studying the propagation error during the composition of geometric transformations one has to have in mind the possibly dependence of input data on each other.

As an example, look at a fat point $P$ in the shape of a disk of radius $r$, which first undergoes the rotation $G(Q_1, \theta_1, 1)$, and then the rotation $G(Q_2, \theta_2, 1)$, defined by fat centers $Q_1, Q_2$, which are themselves disks of radii $r', r''$, respectively. In view of Prop. 6 or more precisely Equ. (8), the resulting tolerance zone is a disk of radius

$$2r'' \,|\sin(\theta_2/2)| + 2r' \,|\sin(\theta_1/2)| + r. \tag{10}$$

The fact that $Q_1 = Q_2$ can have two different interpretations: Maybe the two rotations are independent and their centers, in principle being independent, happen to share the same tolerance zone. But maybe the two centers are meant to be the same point, so the two rotations are no longer independent. Thus we not only have $r' = r''$, but the image of $P$ under their composition is a disk of radius

$$2r' \,|\sin((\theta_1 + \theta_2)/2)| + r. \tag{11}$$

This is in general smaller than the radius which we get by letting $r' = r''$ in Equ. (10).

This example is an instance of the general principle that applying independently defined transformations $G(Q_1, \dots)$ and $G(Q_2, \dots)$ to a fat point $P$ results in the tolerance zone

$$G(Q_2, \dots)(G(Q_1, \dots)(P)), \tag{12}$$

whereas the tolerance zone of the composition is only a subset of (12), if the single transformations are not independent. In this way the relation "(11) $\leq$ (10)" is actually a proof of the inequality

$$|\sin(\alpha + \beta)| \leq |\sin\alpha| + |\sin\beta|. \tag{13}$$

There may be transformations which do not exhibit this behaviour, for example the central similarity transformation: We apply the central similarities with fat centers $Q_1, Q_2$ and factors $\lambda_1$, $\lambda_2$ to the fat point $P$, which results in

$$(1-\lambda_2)Q_2 + \lambda_2((1-\lambda_1)Q_1 + \lambda_1 P).$$

Letting $Q = Q_1 = Q_2$ results in

$$(1-\lambda_1\lambda_2)Q + \lambda_1\lambda_2 P,$$

which is the same as applying the central similarity with center $Q$ and factor $\lambda_1\lambda_2$ to $P$.

## Acknowledgements

This work was supported by the Austrian Science Foundation (Grant No. P15911) and the Natural Science Foundation of China (Project number 60273012).

## References

[1] S.L. Abrams et al: *Efficient and reliable methods for rounded-interval arithmetic*. Computer-Aided Design **30**, 657–665 (1998).

[2] M. Aichinger: *A Collision Problem for Worst Case Tolerance Objects*. Dissertation, Johannes Kepler-Universität Linz, 1996.

[3] P. Ghosh: *A unified computational framework for Minkowski operations*. Computers & Graphics **17**, 357–378 (1993).

[4] C.U. Hinze: *A Contribution to Optimal Tolerancing in 2-Dimensional Computer Aided Design*. Dissertation, Johannes Kepler-Universität Linz, 1994.

[5] C.-Y. Hu, N.M. Patrikalakis, X. Ye: *Robust interval solid modeling*. Computer-Aided Design **28**, 819–830 (1996).

[6] C.-Y. Hu, T. Maekawa, N.M. Patrikalakis, X. Ye: *Robust interval algorithm for surface intersections*. Computer-Aided Design **29**, 617–627 (1997).

[7] C.-Y. Hu, T. Maekawa, E.C. Sherbrooke, N.M. Patrikalakis: *Approximation of measured data with interval B-splines*. Computer-Aided Design **29**, 791–799 (1997).

[8] R. Moore: *Interval Analysis*. Prentice-Hall, 1966.

[9] N. Patrikalakis, T. Maekawa: *Shape Interrogation for Computer-Aided Design and Manufacturing*. Springer 2002.

[10] H. Pottmann, B. Odehnal, M. Peternell, J. Wallner, R. Ait Haddou: *On Optimal Tolerancing in Computer-Aided Design*. Proc. Geometric Modeling and Processing 2000, IEEE CS Press, Hong Kong, 2000; pp. 347–363.

[11] H. Pottmann, J. Wallner: *Computational Line Geometry*. Springer, Berlin 2001.

[12] A.A.G. Requicha: *Towards a theory of geometric tolerancing*. Int. J. of Robotics Research **2**, 45–60 (1983).

[13] T.W. Sederberg, R.T. Farouki: *Approximation by interval Bézier curves*. IEEE Computer Graphics **12**, 87–95 (1992).

[14] G. Shen, N. Patrikalakis: *Numerical and Geometric Properties of Interval B-Splines*. Int. J. Shape Modeling **4**, 31–62 (1998).

[15] J. Wallner, R. Krasauskas, H. Pottmann: *Error propagation in geometric constructions*. Computer Aided Design **32**, 631–641 (2000).

[16] J. Wallner: *On a problem of elementary differential geometry and the number of its solutions*. Technical Report No. 106, Institut für Geometrie, 2003. http://www.geometrie.tuwien.ac.at/wallner/skp.pdf.

Received September 22, 2004